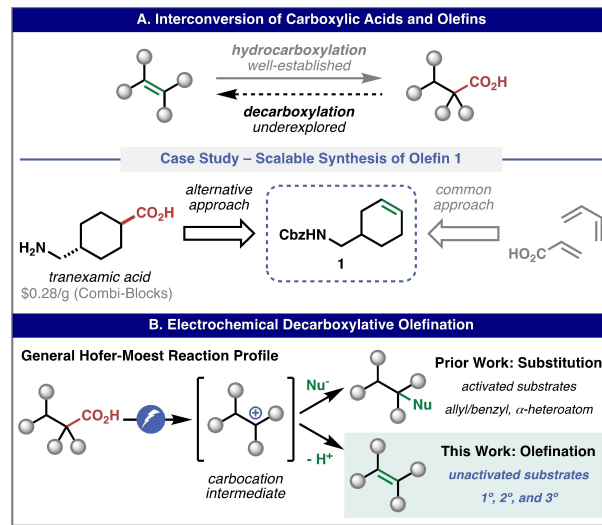


# Scalable Electrochemical Decarboxylative Olefination Driven by Alternating Polarity\*\*

Alberto F. Garrido-Castro, Yuta Hioki, Yoshifumi Kusumoto, Kyohei Hayashi, Jeremy Griffin, Kaid C. Harper, Yu Kawamata,\* and Phil S. Baran\*

**Abstract:** A mild, scalable (kg) metal-free electrochemical decarboxylation of alkyl carboxylic acids to olefins is disclosed. Numerous applications are presented wherein this transformation can simplify alkene synthesis and provide alternative synthetic access to valuable olefins from simple carboxylic acid feedstocks. This robust method relies on alternating polarity to maintain the quality of the electrode surface and local pH, providing a deeper understanding of the Hofer-Moest process with unprecedented chemoselectivity.

The incorporation of carboxyl groups onto olefins is one of the most useful and industrially applied reactions of the modern era (e.g., hydrocarboxylation, Figure 1A).<sup>[1-4]</sup> The reverse process of removing a carbonyl group (deformylation/decarboxylation) is less studied, yet could serve as a convenient tool to install an olefin when the carboxylic acid is readily available, offering alternative disconnections for retrosynthetic analysis.<sup>[5-7]</sup> For example, olefin **1** could be envisioned to arise from a sequence of Diels–Alder<sup>[8]</sup> and functional group manipulations<sup>[9]</sup> or, perhaps more attractively, from readily available tranexamic acid in a single operation (following Cbz protection). One potential plat-



**Figure 1.** Interconversion of carboxylic acids and olefins. (A) Whereas hydrocarboxylation is well-established on industrial scale, decarboxylative olefination remains underexplored despite its synthetic value. (B) Electrochemical oxidation of carboxylic acids can invoke Hofer-Moest reactivity.

[\*] A. F. Garrido-Castro, Y. Hioki, Y. Kusumoto, K. Hayashi, Y. Kawamata, P. S. Baran  
Department of Chemistry, Scripps Research  
10550 North Torrey Pines Road, La Jolla, CA 92037 (USA)  
E-mail: yukawama@scripps.edu  
pbaran@scripps.edu

A. F. Garrido-Castro  
Laboratorium für Organische Chemie, ETH Zürich  
Vladimir-Prelog-Weg 3, HCI, 8093 Zürich (Switzerland)

Y. Hioki  
Science and Innovation Center, Mitsubishi Chemical Corporation  
1000, Kamoshida-cho, Aoba-ku, Yokohama, Kanagawa 227-8502  
(Japan)

J. Griffin, K. C. Harper  
AbbVie Process Research and Development  
1401 North Sheridan Road, North Chicago, IL 60064 (USA)

[\*\*] A previous version of this manuscript has been deposited on a preprint server (<https://doi.org/10.26434/chemrxiv-2023-49z1z>).

© 2023 The Authors. Angewandte Chemie International Edition published by Wiley-VCH GmbH. This is an open access article under the terms of the Creative Commons Attribution License, which permits use, distribution and reproduction in any medium, provided the original work is properly cited.

form to access this reactivity would be via an electrochemically generated carbocation produced by decarboxylation (Figure 1B). Such reactivity is embodied by the classic Hofer-Moest reaction,<sup>[6,10-13]</sup> a transformation that generates these reactive intermediates through a strongly oxidative process. Although there are numerous examples that utilize this electrosynthetic tactic, the vast majority proceed only on activated systems (allylic, benzylic, and  $\alpha$ -heteroatom).<sup>[14]</sup> Recent variants, such as decarboxylative etherification<sup>[14]</sup> and fluorination,<sup>[15]</sup> have extended the scope of this reaction largely to tertiary systems and select secondary examples. Electrochemical decarboxylation of secondary, let alone primary carboxylic acids, is considered extremely challenging even in these state-of-the-art protocols. The recently developed rapid alternating polarity (rAP)<sup>[16,17]</sup> variant of the Kolbe reaction is a notable exception as it enables decarboxylation of primary carboxylic acids with high chemoselectivity;<sup>[18]</sup> however, this reaction favors carbon radical formation over the carbocation. To the best of our knowledge, a general electrochemical decarboxylative olefination has yet to be described. In this communication, we disclose a modification of the rAP-Kolbe conditions, now allowing facile decarboxylation of unactivated primary,

secondary, and tertiary carboxylic acids without the need for preactivation (e.g., redox-active ester formation), enabling access to olefins via carbocations.

Our preliminary studies started from slightly modified electrochemical decarboxylations for etherification<sup>[14]</sup> and fluorination<sup>[15]</sup> (Table 1). In an attempt to favor olefination, the alcohol nucleophile was excluded from the etherification conditions (entry 1). However, oxidation of the model secondary acid was sluggish, and no olefin product was observed. Fluorination conditions led to trace conversion to olefin **1**, in good agreement with the original report that this method is not applicable to secondary carboxylic acids (entry 2). rAP-Kolbe conditions<sup>[18]</sup> gave much better conversion when compared to the previous methods, resulting in moderate yield of **1** (entry 3). To further improve the reaction, graphite electrodes were evaluated based on their well-established ability to access carbocations over carbon radicals.<sup>[11,19]</sup> However, switching to graphite electrodes resulted in low conversion with 50 ms rAP (entry 4). This large drop in conversion could be explained by the order of magnitude higher electrode capacitance of graphite over reticulated vitreous carbon (RVC), i.e., electricity was largely consumed by charge–discharge cycles of the electrical double layer. An estimation of the electrode capacitance for graphite and RVC electrodes can be found in our previous work.<sup>[16a]</sup> To account for such a large electrode capacitance, a much longer pulse was applied (5 s instead of 50 ms), resulting in a significant improvement in conversion and 67% yield of the desired olefin (entry 5). The rest of the mass balance could be attributed to other Hofer-Moest byproducts formed by addition of a nucleophile such as carboxylate or water, while no Kolbe coupling products were observed. These conditions compare to state-of-the-art

photochemical methods (entries 6 and 7),<sup>[20]</sup> and as illustrated below, this functional electrochemical protocol enables unprecedented scalability (up to 1 kg) in the context of decarboxylative olefination of unactivated carboxylic acids. Remarkably, these optimized conditions did not work (on preparative scale) if direct current (DC) electrolysis was applied instead of alternating polarity. In fact, no conversion was observed under DC conditions (entry 8, see mechanistic studies below). A catalytic amount of base is necessary to ensure conversion of carboxylic acid **2** (entry 9). Use of tetramethylammonium salts can be circumvented by replacement with KOH (entry 10). Furthermore, the addition of pivalic acid is necessary to avoid partial oxidative degradation of the olefin product (entry 11). 2-Methyl-2-butene can also be used in place of pivalic acid (entry 12), further confirming the role of PivOH as a sacrificial additive rather than a pH buffering agent due to its acidic nature.

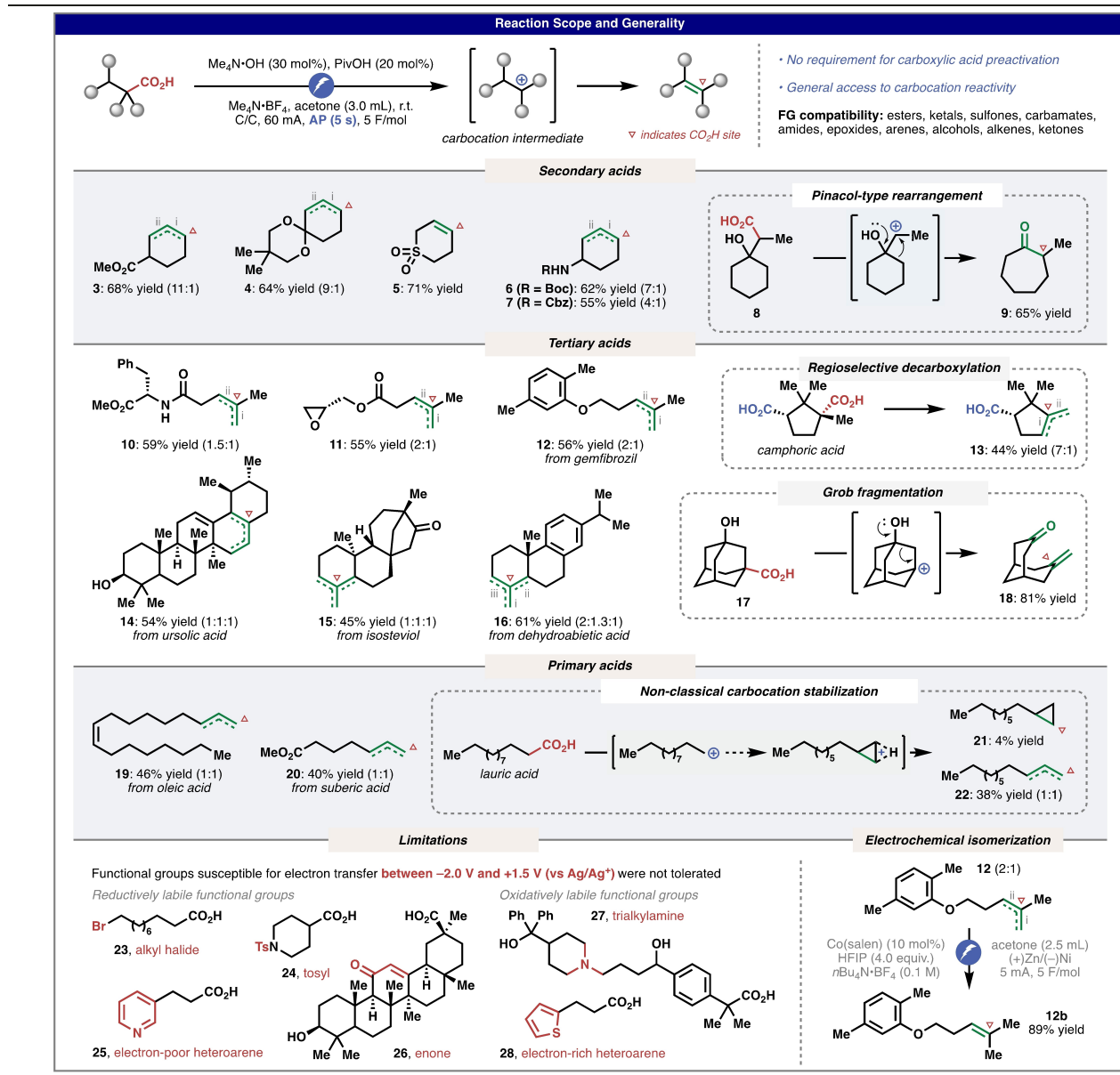
With optimized conditions in hand, the scope of this electrochemical decarboxylative olefination was explored. In general, this practical method is applicable to a variety of unactivated secondary, tertiary, and even primary carboxylic acids as illustrated in Table 2. Compatible functional groups include: esters (**3**, **10**, **11**, **20**), ketals (**4**), sulfones (**5**), carbamates (**6**, **7**), amides (**10**), epoxides (**11**), arenes (**12**, **16**), alcohols (**14**, **19**) and ketones (**15**). As demonstrated in **3–7**, this method offers rapid access to unsaturated six-membered rings with a variety of functional groups. Although such a motif is a prime target for Diels–Alder approaches, accessibility and stability of the reactants, as well as polarity matching, is not always trivial. For example, access to olefinic sulfone **5** can be laborious (previously reported in 7 steps),<sup>[21]</sup> whereas electrochemical decarboxylation allows its preparation in a single step from the commercially available acid (\$5.4/g). Similarly, the synthesis of 4-aminocyclohexene derivatives **6** and **7** from a readily available carboxylic acid (\$4.8/g, free amine) also exemplifies the potential of this protocol to circumvent a cumbersome Diels–Alder/Curtius rearrangement sequence.<sup>[8,22]</sup> Medicinally relevant gemfibrozil, used as a lipid regulator to treat high cholesterol, offers an intriguing case study on chemoselectivity. The electron-rich alkyl aryl ether prone to electrochemical oxidation was tolerated in the decarboxylative olefination, highlighting the chemoselective nature of the oxidation process. The method also allows facile derivatization of naturally occurring carboxylic acids such as ursolic acid, isosteviol, and dehydroabietic acid to deliver unique olefins with complex polycyclic scaffolds (**14–16**). Interestingly, in the case of camphoric acid, the tertiary acid was selectively decarboxylated to afford  $\gamma,\delta$ -unsaturated acid **13**. Simple primary carboxylic acids—the most abundant yet least prone to undergo Hofer-Moest—are efficiently decarboxylated under this protocol. Oleic acid, a common component of plant oil, can be turned into an exotic diene **19**, while suberic acid monomethyl ester can be converted into a valuable unsaturated ester **20** (\$160/g). In addition to olefin product formation, this protocol demonstrates different reaction outcomes based on the nature of the carbocation intermediate.  $\beta$ -Hydroxy acid **8** can readily undergo decarboxylation followed by pinacol-

**Table 1:** Discovery of the electrochemical decarboxylative olefination. Benchmarks with state-of-the-art conditions and effect of key reaction parameters (see Supporting Information for further details). i and ii indicate olefin regioisomers.

Reaction Discovery and Benchmarks			
Entry	Transformation	Reaction conditions	Conv. (%) <sup>[a]</sup> Yield (%) <sup>[a]</sup>
1	Decarboxylative etherification (ref 14)	collidine, AgPF <sub>6</sub> , nBu <sub>4</sub> N·PF <sub>6</sub> , 3 Å MS DCM, r.t., (+)C/(-)C, 10 mA	59 n.d.
2	Decarboxylative fluorination (ref 15)	collidinium-BF <sub>4</sub> , collidine, 3 Å MS DCM, r.t., (+)C/(-)C, 36.2 mA	35 trace
3	rAP Kolbe (ref 18)	Me <sub>4</sub> N·OH (10 mol%), acetone, r.t. RVC/RVC, 60 mA, rAP (50 ms)	94 36
4	rAP Kolbe variant	same as entry 3, C/C instead of RVC/RVC	15 3
5	This work	Me <sub>4</sub> N·OH (30 mol%), PivOH (20 mol%) Me <sub>4</sub> N·BF <sub>4</sub> , acetone, r.t., C/C, 60 mA, AP (5 s)	>98 67
6	Co/Ir hν (ref 20a)	[Co] cat., [Ir] cat., Cs <sub>2</sub> CO <sub>3</sub> DME:H <sub>2</sub> O (18:1), blue LEDs, r.t.	67 22 <sup>[b]</sup>
7	Co/acridine hν (ref 20b)	[Co] cat., acridine MeCN:DCM (2:1), purple LEDs, r.t.	>98 55 <sup>[b]</sup>
Effect of Reaction Parameters under Conditions in Entry 5			
8	DC electrolysis instead of AP (5 s)		9 n.d.
9	no Me <sub>4</sub> N·OH		20 n.d.
10	KOH instead of Me <sub>4</sub> N·OH, no Me <sub>4</sub> N·BF <sub>4</sub>		>98 59
11	no PivOH		>98 41
12	2-methyl-2-butene instead of PivOH		>98 64

[a] Determined by <sup>1</sup>H NMR. [b] Obtained as single isomer i.

**Table 2:** Scope of the electrochemical decarboxylative olefination. Diverse examples of carbocation reactivity and limitations are shown, as well as the possibility to obtain a single olefin isomer. i, ii, and iii indicate olefin regioisomers; ratio is determined by <sup>1</sup>H NMR.



type rearrangement to form cyclic ketone **9**,<sup>[23]</sup> while adamantan derivative **17** efficiently leads to Grob fragmentation product **18**.<sup>[15]</sup> Another unique evidence of carbocation intermediacy was obtained in the decarboxylation of a primary acid, where the formation of alkene **22** was accompanied by cyclopropane **21**. This byproduct formation invokes a non-classical carbocation stabilization followed by a new C–C  $\sigma$ -bond formation via  $\gamma$ -deprotonation.<sup>[24–26]</sup> Since oxidative decarboxylation is balanced by reduction of acetone used as solvent, confirmed by the detection of  $\approx 1.0$  equiv. of isopropanol in crude <sup>1</sup>H NMR (see SI), functional groups susceptible to electron-transfer within the redox window of carboxylate and acetone might not be tolerated (Table 2, bottom left).<sup>[27]</sup> Therefore, reductively labile functionalities such as alkyl halides (**23**), aryl sulfonamides (**24**), electron-poor heterocycles (**25**), or enones (**26**) were not amenable to the current reaction conditions. Similarly, tertiary alkyl amines (**27**) or electron-rich heterocycles (**28**) interfered with oxidative decarboxylation. In certain cases, olefin formation provided an inseparable mixture of isomers. In this scenario, the mixture could be converted into a single product by enlisting alkene isomerization conditions (Table 2, bottom right), using the recently reported electrocatalytic generation of Co–H to access the internal isomer **12b**.<sup>[28,29]</sup>

The ultimate proving ground for this simple, metal-free protocol is in its applicability to be conducted on a large scale. Thus, we partnered with AbbVie process chemists to scale the electrochemical decarboxylative olefination of carboxylic acid **2** (Figure 2). Translation of the method to

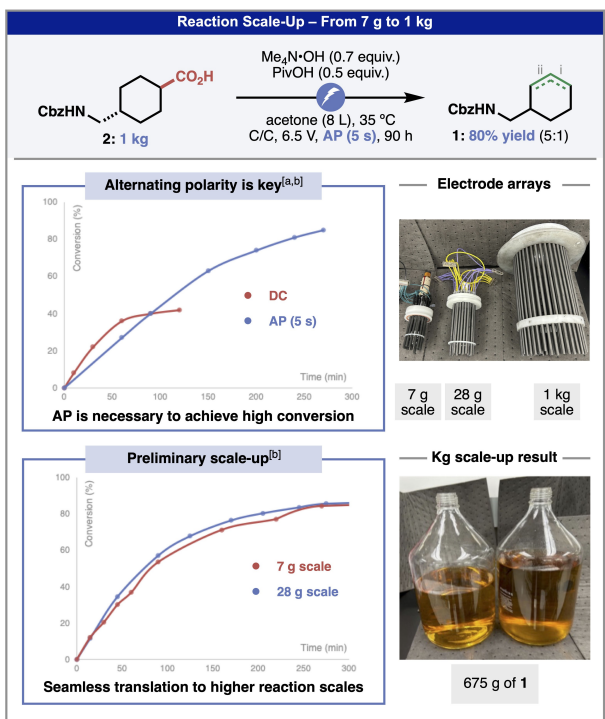


**Figure 2.** Electrochemical decarboxylative olefination scale-up developed at AbbVie. Process was seamlessly scaled-up from 7 g to 1 kg. Alternating polarity is shown to be necessary to avoid the reaction stalling. <sup>[a]</sup> 7 g scale. <sup>[b]</sup> Reactions monitored by HPLC.

the continuous stirred-tank reactor (CSTR), employing a cylindrical electrode array (Figure 2, top right), was straightforward. Equivalents of base and sacrificial additive were modified, and the electrolysis mode was switched from constant current to constant potential, to maximize the current and minimize reaction time. Since the AbbVie reactor (see SI) allows facile optimization of reaction temperature, it was fine-tuned to 35 °C. Overall, in less than 10 lab experiments on 7 g scale, suitable conditions were identified for scale-up. Notably, achieving high conversion was challenging under DC electrolysis despite moderate starting material consumption (Figure 2, top left), confirming that the importance of alternating polarity is universal across various reaction scales. Increasing the scale of the reaction from 7 to 28 g in a larger reactor led to nearly identical reaction performance (Figure 2, bottom left). This preliminary scale-up effort successfully demonstrated that scaling the reaction based on electrode surface area would lead to predictable results. Thus, further scale-up to 1 kg was undertaken by simply using a larger electrode array (Figure 2, top right). The surface area of this electrode array supposes a ten-fold increase relative to the array used for the 28 g reaction and fits into an 8 L reactor body. To achieve a batch reaction size of 1 kg in this reactor, the reaction was further concentrated from  $\approx 0.25$  M under the nominal conditions to 0.8 M without consequence. The next hurdle to be addressed was identifying equipment capable of providing alternating polarity current. The expected current flow for a 1 kg reaction would be in excess of 100 A;

however, no power source capable of supplying this amperage with polarity alternation was readily available on the market. Therefore, a lab potentiostat capable of a 20 A maximum output was used as a compromise. The elevated capacitance of the graphite electrode material presented an additional challenge, which was addressed by designing a custom step-down reversal of polarity (see Supporting Information for further details). Despite the equipment limitation resulting in a longer reaction time (90 hours), the kg-scale reaction proceeded smoothly, providing a comparable 80 % isolated yield of olefin **1** (Figure 2, bottom right). The reaction could be amenable to flow conditions owing to consistent performance across different scales. To place these results in context, a hypothetical cost comparison of an analogous photochemical variant<sup>[20a]</sup> is put forth, wherein the electrochemical reaction would require \$89 for all the reagents to provide 675 g of **1** (\$26/mol of **1**), while the Ir catalyst alone would cost  $> \$1,000$  (\$302/mol of **1**)<sup>[30]</sup> on the same reaction scale. A more cost-effective acridine-catalyzed photochemical variant<sup>[20b]</sup> is confined to small scale synthesis, and in order to access grams of product the reaction has to be set up many times in parallel.

Alternating polarity (AP) every 5 seconds and DC electrolysis usually share similar reactivity profiles;<sup>[31]</sup> therefore, it is of great surprise that merely switching from AP to DC results in little conversion under otherwise identical conditions (Table 1, entry 8). Accordingly, preliminary mechanistic investigations were conducted to provide a deeper understanding on the effect of AP on this transformation (Figure 3). The most notable visual difference between the reactions with and without AP was the appearance of electrodes after completion of the electrolysis (Figure 3A). While the appearance of the electrodes under AP conditions remained unaltered, the anode surface of the DC experiment electrodes had clearly been compromised. Moreover, electrode weight was monitored before and after electrolysis, observing non-negligible mass gain only on the DC anode, further supporting irreversible anode fouling. It was reasoned that such anode fouling occurs due to the depletion of oxidizable substance on the anode. This situation is comparable to the rAP-Kolbe reaction, where smooth decarboxylation only under rAP conditions could be explained by a local pH difference around the electrodes.<sup>[18]</sup> Namely, DC electrolysis generates locally acidic areas around the anode through the formation of electrogenerated acids,<sup>[32]</sup> which suppresses deprotonation of carboxylic acid, and therefore, decarboxylation. In contrast, polarity switching can partially avert this phenomenon by reversing electrode polarity, thus diminishing the accumulation of acid around the electrode. In order to support this hypothesis, probe **30** bearing an acid-labile silyl ether functionality was introduced into the reactions (Figure 3B, top panel). While DC electrolysis generated the deprotected alcohol **31** in 33 % yield, only 10 % of **31** was detected under AP conditions. This supports the notion that AP attenuates local pH fluctuation. Furthermore, cyclic voltammetry (CV) studies clearly indicate the lack of an oxidation event without adding a base (Figure 3B, bottom panel), which could lead to high potential at the electrode and result in

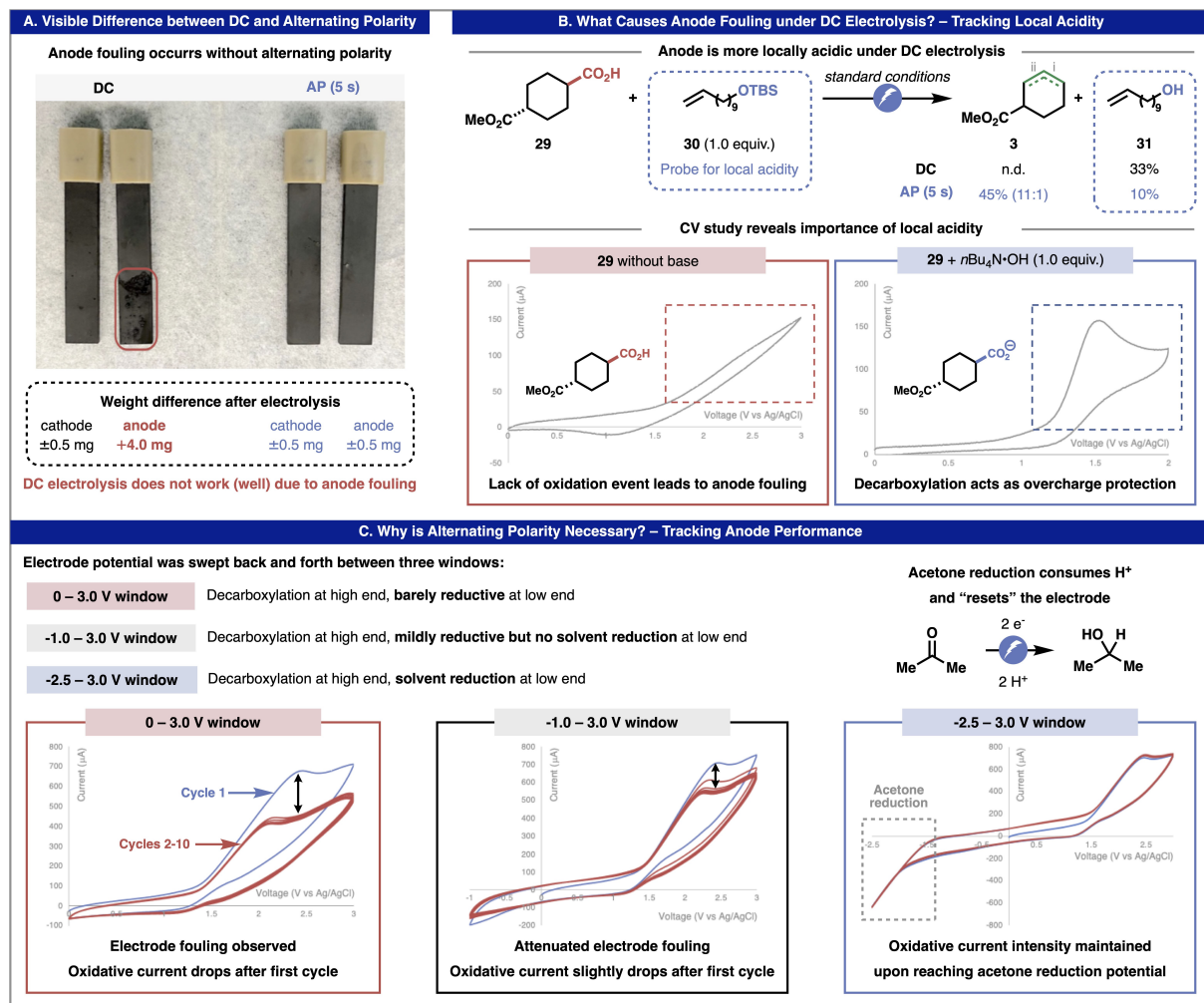


**Figure 3.** Mechanistic studies on the electrochemical decarboxylative olefination. (A) Visible difference between DC and alternating polarity, (B) tracking local acidity to explain the cause for anode fouling under DC electrolysis, and (C) tracking anode performance to explain the need for alternating polarity.

anode fouling. On the other hand, CV of carboxylic acid **29** in the presence of base exhibits an oxidation peak around 1.5 V, which is in good agreement with the reported oxidation potential of alkyl carboxylates.<sup>[27]</sup> This oxidation event could be acting as overcharge protection, thus maintaining the integrity of the electrodes throughout the reaction. Following the acidity study highlighted in Figure 3B, further CV studies were undertaken to provide a more detailed analysis on the impact of AP on this decarboxylative process (Figure 3C). In order to replicate the reaction process as closely as possible, a graphite electrode was used as working electrode, and potential was swept for 10 cycles between +3 V and different low ends. Three values were chosen for the low end: 0 V (barely reductive), -1.0 V (reductive, but no solvent reduction), and -2.5 V (sufficiently reductive for solvent reduction to occur). Notably, in the +3–0 V window, the oxidative current intensity dropped considerably after the first cycle, possibly indicating electrode fouling. Lowering the reductive end of the window to -1.0 V attenuated this current drop.

Upon reaching -2.5 V, a new reductive event associated with acetone reduction was observed, and the oxidative current intensity was maintained during ten cycles. This result indicates that the reduction of acetone, which consumes protons, is crucial to support smooth decarboxylation over time, thus resupplying carboxylate species for further oxidation. Based on the observation of isopropanol in crude <sup>1</sup>H NMR on preparative scale, this scenario likely explains the role of AP. Namely, local acidity caused by electrogenerated acid renders the oxidative decarboxylation sluggish and eventually halted under DC electrolysis. On the other hand, polarity switching can replenish carboxylate by the reduction of acetone, which acts as sacrificial electron- and proton-acceptor.

To summarize, a simple protocol for decarboxylative olefination is presented which precludes the need for expensive catalysts, ligands, additives, or any metals. The closest alternative methods to this transformation are photochemical decarboxylative olefinations, which are either cost-prohibitive or limited to small scale synthesis. Indeed, the

scalability of this electrochemical reaction is vividly illustrated by the facile execution of a 1 kg scale reaction to provide a pharmaceutically relevant molecule. The chemoselectivity observed allows access to a range of olefins starting from ubiquitous, unactivated carboxylic acids. Mechanistic investigations highlight the critical role of local pH around electrodes—an overlooked phenomenon in the context of Hofer-Moest reactivity. More broadly, this work represents another example of how alternating polarity regimes in electrosynthesis hold promise for the improvement and invention of useful, practical, and sustainable transformations where electrons are the primary reagent.

### Acknowledgements

This work was supported by National Science Foundation Center for Synthetic Organic Electrochemistry CHE-2002158 (reaction development and optimization) and AbbVie (scale-up). A.F.G.-C. thanks the European Commission for a Marie Skłodowska-Curie Global Fellowship (H2020-MSCA-IF-2020-GF-101027337-CatToSat). Y.K. (third author) acknowledges financial support from Shionogi & Co., Ltd during this work. We thank Dr. D.-H. Huang and Dr. L. Pasternack (Scripps Research) for assistance with NMR spectroscopy, Dr. J. Chen, B. Sanchez, Q. Nguyen, and E. Sturgell (Scripps Automated Synthesis Facility) for assistance with LCMS and HRMS. We also thank Dr. Pierre-Georges Echeverria, Dr. Manolis Sofiadis, Dr. You-Chen Lin, Dr. Gabriele Laudadio, Dr. Molhm Nassir, Prof. Samer Gnaim, Dr. Nathanyal Truax, Alexandros Pollatos and Simona Kotesova for helpful discussions as well as Melania Prado Merini, Dr. Shing Bong Lou and Dr. Matteo Costantini for early explorations.

All data are available in the main text or Supporting Information.

### Conflict of Interest

K.C.H. and J.G. are employees of AbbVie and may own AbbVie stock. Y.H., Y.K. and P.S.B. are the inventors of US patent application no. 63/352,091, which includes the transformation described herein.

### Data Availability Statement

The data that support the findings of this study are available in the supplementary material of this article.

**Keywords:** Decarboxylation · Electrochemistry · Olefination · Reaction Mechanisms · Synthetic Methods

[1] C. Schneider, T. Leischner, P. Ryabchuk, R. Jackstell, K. Junge, M. Beller, *CCS Chem.* **2021**, *3*, 512–530.

- [2] X.-F. Wu, H. Neumann, M. Beller, *ChemSusChem* **2013**, *6*, 229–241.
- [3] S.-S. Yan, Q. Fu, L.-L. Liao, G.-Q. Sun, J.-H. Ye, L. Gong, Y.-Z. Bo-Xue, D.-G. Yu, *Coord. Chem. Rev.* **2018**, *374*, 439–463.
- [4] Y.-X. Luan, M. Ye, *Tetrahedron Lett.* **2018**, *59*, 853–861.
- [5] a) B. M. Stadler, C. Wulf, T. Werner, S. Tin, J. G. de Vries, *ACS Catal.* **2019**, *9*, 8012–8067; F. J. Holzhäuser, J. B. Mensah, R. Palkovits, *Green Chem.* **2020**, *22*, 286–301; b) U. Biermann, U. T. Bornscheuer, I. Feussner, M. A. R. Meier, J. O. Metzger, *Angew. Chem. Int. Ed.* **2021**, *60*, 20144–20165.
- [6] For a conceptually different approach involving metal-catalyzed decarbonylation of activated acids, see: a) J. A. Miller, J. A. Nelson, M. P. Byrne, *J. Org. Chem.* **1993**, *58*, 18–20; b) S. Maetani, T. Fukuyama, N. Suzuki, D. Ishihara, I. Ryu, *Organometallics* **2011**, *30*, 1389–1394; c) S. Maetani, T. Fukuyama, N. Suzuki, D. Ishihara, I. Ryu, *Chem. Commun.* **2012**, *48*, 2552–2554; d) A. John, M. O. Miranda, K. Ding, B. Dereli, M. A. Ortúño, A. M. LaPointe, G. W. Coates, C. J. Cramer, W. B. Tolman, *Organometallics* **2016**, *35*, 2391–2400.
- [7] For biocatalytic decarboxylative methods, see: R. Wohlgemuth, *ChemSusChem* **2022**, *15*, e202200402.
- [8] F. X. Werber, J. E. Jansen, T. L. Gresham, *J. Am. Chem. Soc.* **1952**, *74*, 532–535.
- [9] S. Hailong, W. Yanyu, G. Yilong, C. Xinhua, M. Jun, L. Na, K. Lin, B. Jiye, C. Shaohui, Y. Aiwu, X. Yuexing, (China Petroleum and Chemical Corp, Sinopec Yangzi Petrochemical Co Ltd), CN104557357 A, **2014**.
- [10] V. Ramadoss, Y. Zheng, X. Shao, L. Tian, Y. Wang, *Chem. Eur. J.* **2021**, *27*, 3213–3228.
- [11] M. C. Leech, K. Lam, *Acc. Chem. Res.* **2020**, *53*, 121–134.
- [12] S.-H. Shi, Y. Liang, N. Jiao, *Chem. Rev.* **2021**, *121*, 485–505.
- [13] M. Yan, Y. Kawamata, P. S. Baran, *Chem. Rev.* **2017**, *117*, 13230–13319.
- [14] J. Xiang, M. Shang, Y. Kawamata, H. Lundberg, S. H. Reisberg, M. Chen, P. Mykhailiuk, G. Beutner, M. R. Collins, A. Davies, M. D. Bel, G. M. Gallego, J. E. Spangler, J. Starr, S. Yang, D. G. Blackmond, P. S. Baran, *Nature* **2019**, *573*, 398–402. For a compilation of Hofer-Moest examples, please see Supporting Information within.
- [15] M. C. Leech, D. Nagornii, J. M. Walsh, C. Kiaku, D. L. Poole, J. Mason, I. C. A. Goodall, P. Devo, K. Lam, *Org. Lett.* **2023**, *25*, 1353–1358.
- [16] a) Y. Kawamata, K. Hayashi, E. Carlson, S. Shaji, D. Waldmann, B. J. Simmons, J. T. Edwards, C. W. Zapf, M. Saito, P. S. Baran, *J. Am. Chem. Soc.* **2021**, *143*, 16580–16588; b) K. Hayashi, J. Griffin, K. C. Harper, Y. Kawamata, P. S. Baran, *J. Am. Chem. Soc.* **2022**, *144*, 5762–5768.
- [17] For reviews on the use of alternating current in organic synthesis, please see: a) S. Rodrigo, D. Gunasekera, J. P. Mahajan, L. Luo, *Curr. Opin. Electrochem.* **2021**, *28*, 100712; b) J. Zhong, C. Ding, H. Kim, T. McCallum, K. Ye, *Green Synth. Catal.* **2022**, *3*, 4–10; c) M. Jamshidi, C. Fastie, G. Hilt, *Synthesis* **2022**, *54*, 4661–4672.
- [18] Y. Hioki, M. Costantini, J. Griffin, K. C. Harper, M. P. Merini, B. Nissl, Y. Kawamata, P. S. Baran, *Science* **2023**, *380*, 81–87.
- [19] H. J. Schäfer, *Chem. Phys. Lipids* **1979**, *24*, 321–333.
- [20] a) X. Sun, J. Chen, T. Ritter, *Nat. Chem.* **2018**, *10*, 1229–1233; b) V. T. Nguyen, V. D. Nguyen, G. C. Haug, H. T. Dang, S. Jin, Z. Li, C. Flores-Hansen, B. S. Benavides, H. D. Arman, O. V. Larionov, *ACS Catal.* **2019**, *9*, 9485–9498.
- [21] R. M. Chabanenko, S. Y. Mykolenko, E. K. Kozirev, V. A. Palchykov, *Synth. Commun.* **2018**, *48*, 2198–2205.
- [22] J. R. Pfister, W. E. Wymann, *Synthesis* **1983**, *1983*, 38–40.
- [23] Z. Zhang, L. Zhang, X. Zhang, J. Yang, Y. Yin, Y. Jiang, C. Zeng, G. Lu, Y. Yang, F. Mo, *Chem. Sci.* **2020**, *11*, 12021–12028.

[24] G. J. Karabatsos, N. Hsi, S. Meyerson, *J. Am. Chem. Soc.* **1970**, *92*, 621–626.

[25] P. S. Grant, R. Meyrelles, O. Gajsek, G. Niederacher, B. Maryasin, N. Maulide, *J. Am. Chem. Soc.* **2023**, *145*, 5855–5863.

[26] P. J. Kropp, R. L. Adkins, *J. Am. Chem. Soc.* **1991**, *113*, 2709–2717.

[27] H. Roth, N. Romero, D. Nicewicz, *Synlett* **2015**, *27*, 714–723.

[28] S. Gnaim, A. Bauer, H.-J. Zhang, L. Chen, C. Gannett, C. A. Malapit, D. E. Hill, D. Vogt, T. Tang, R. A. Daley, W. Hao, R. Zeng, M. Quertenmont, W. D. Beck, E. Kandahari, J. C. Vantourout, P.-G. Echeverria, H. D. Abruna, D. G. Blackmond, S. D. Minteer, S. E. Reisman, M. S. Sigman, P. S. Baran, *Nature* **2022**, *605*, 687–695.

[29] S. W. M. Crossley, F. Barabé, R. A. Shenvi, *J. Am. Chem. Soc.* **2014**, *136*, 16788–16791.

[30] Price for bulk Ir metal was used as a cheapest source of Ir for cost comparison: <https://www.dailymetalprice.com/metalprices.php> (accessed May 1 2023).

[31] G. Hilt, *ChemElectroChem* **2020**, *7*, 395–405.

[32] M. F. Nielsen, *Encyclopedia of Electrochemistry*, Wiley-VCH, Weinheim, **2007**, p. 451.

Manuscript received: June 28, 2023

Accepted manuscript online: September 1, 2023

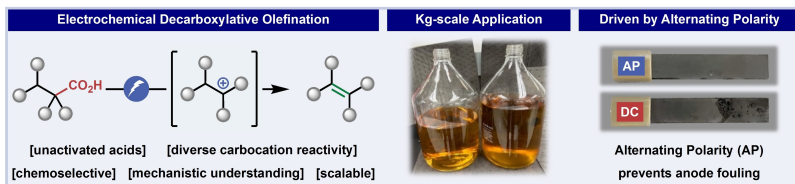
Version of record online: ■■■

## Communications

## Alkenes

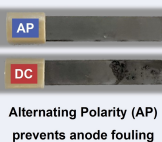
A. F. Garrido-Castro, Y. Hioki, Y. Kusumoto, K. Hayashi, J. Griffin, K. C. Harper, Y. Kawamata,\* P. S. Baran\* – e202309157

## Scalable Electrochemical Decarboxylative Olefination Driven by Alternating Polarity



## Kg-scale Application

## Driven by Alternating Polarity



Alternating Polarity (AP) prevents anode fouling

The electrochemical conversion of unactivated carboxylic acids to olefins under alternating polarity is reported. By modulating electrode surface quality and local acidity, chemoselective Hofer-Moest reactivity is realized on convention-

ally difficult substrates, including primary and secondary unactivated carboxylic acids. This simple protocol is exceptionally scalable (1 kg) and cost-effective.